492

Proposal to Construct an Antiproton Source for the Fermilab Accelerators

D. Cline, P. McIntyre, D. D. Reeder, C. Rubbia and L. Sulak

Department of Physics
Harvard University
Cambridge, Massachusetts 02138

Department of Physics
University of Wisconsin
Madison, Wisconsin 53706

M. A. Green, E. M. Rowe, W. S. Tryeciah and W. Winter

Physical Sciences Laboratory
University of Wisconsin
Madison, Wisconsin 53706

Abstract

We propose to build a small storage ring for the accumulation of antiprotons produced in an external target. Stochastic and electron cooling will be used to reduce the transverse and longitudinal phase space of the antiprotons. The dynamics of stochastic and electron cooling will also be studied in this storage ring using circulating protons. The cooled antiprotons can be reinjected into the main ring or energy doubler ring; after simultaneous acceleration along with a proton bunch the accelerator will become a colliding $\bar{p}p$ machine with a center of mass energy range of 300-2600 GeV. Luminosities in the range 10^{29} - 10^{32} $cm^{-2}sec^{-1}$ are expected.

Contents

Introduction

The technological advances in the understanding of the cooling of the transverse and longitudinal phase space of R.F. bunched[1,2,3,4] beams as well as the availability of an intense source of anti-protons at Fermilab, the Fermilab main ring and Energy Doubler ring, have encouraged us to explore once again the old question of building a proton anti-proton storage ring. The physics possibilities of such storage rings operating in the 300-2600 GeV center of mass range are truly enormous. Near the top of the list of physics possibilities is certainly the production and observation of the W° intermediate vector boson through the process

$$\bar{p} + p \to W^\circ + X$$
$$\to \mu^+ + \mu^-$$

However, the collision of intense beams of matter and antimatter at extremely high center of mass energies is more than likely to involve completely undreamed of physics. We therefore think the physics frontier is justification enough for such a venture. In our feasibility study, although not entirely complete, we have uncovered no conceptual problems to building such a machine at Fermilab. The cost of the $\bar{p}$ cooling ring is modest on the scale of planned storage rings. We therefore propose that this machine be constructed at the earliest possible date at Fermilab and that one or more long straight sections be instrumented for physics experiments. The proposal submitted at this time focusses on the conceptual design of this machine. A more complete proposal for the construction of the cooling ring will be submitted in the near future.

2. Physics in Hadron - Anti-hadron Collisions

The possibilities of observing the production and decay of a very high mass (∿100 GeV) intermediate vector boson are reason enough to construct such a machine. In addition for the highest energy option the average parton-antiparton collision has an energy in excess of the weak interaction unitarity limit, therefore the ultimate nature of weak interaction may be decided with this machine.

The study of purely hadronic $\bar{p}p$ interactions will be of great interest. For example the measurement of the total $\bar{p}p$ cross section at such high energies will surely be of interest. However it would be of no use to further catalouge the physics projects since the most interesting discovery to be made would almost certainly not appear on any list made at this time. This is, in fact, the main reason for building the machine.

3. General Scheme for Collecting and Cooling Anti-protons

The general scheme for obtaining a high intensity, cooled antiproton beam is as follows:

1. 3.5 GeV/c antiprotons are produced by an intense, R.F. bunched beam from the main accelerator. The beam energy should be above 50 GeV but need not be above 100 GeV.
2. The $\bar{p}$'s are transported into the accumulator ring by a special transport system that matches the phase space.
3. The antiproton bunch is initially cooled in transverse and longitudinal phase space by stochastic cooling similar to that operated at the ISR.
4. The $\bar{p}$ bunch is moved into a parking orbit and another

$\bar{p}$ bunch is injected. This operation is carried out ~ few thousand times yielding 10^{10}-10^{12} antiprotons.

5. The antiprotons are decelerated to a momentum of 350 MeV/c. Stochastic cooling keeps the beam stable.

6. An intense electron beam is turned on with the electrons traveling with the same velocity as the $\bar{p}$ and in the same direction. Approximately 1 amp/cm^2 is used. The antiproton beam phase space is cooled further to a very small value.

7. The antiproton beam is accelerated up to 9.0 GeV/c.

8. The antiprotons are extracted into a transport system and carried back to the main ring.

9. The $\bar{p}$ are injected into the main ring and a pulse of 5×10^{10} - 5×10^{12} protons are obtained in the main ring and all accelerated up to 50 GeV/c.

10. For higher luminosity ($\sim 10^{30}$-10^{31}cm^{-2}sec^{-1}) requirements some additional R. F. bunching is required.

11. The p and $\bar{p}$ are accelerated to 200 GeV and collide at one or more long straight sections.

12. For operation of the energy doubler as a $\bar{p}p$ storage ring the $\bar{p}$ are first accelerated to 400 GeV/c and transferred to the energy doubler and coast in the "normal" direction. Protons are injected into the main ring, accelerated through transition, R. F. bunched (optional) accelerated to 400 GeV/c and injected into the energy doubler. The $\bar{p}$ and p beams are then accelerated to 1000-1300 GeV/c and collide. The main ring continues to

operate normally and continues to fill the $\bar{p}$ cooling ring for the next injection.

Before discussing in detail the scheme for cooling the transverse and longitudinal oscillations of the $\bar{p}$ beam we first briefly review the status of the theory for the cooling of massive particle beams in storage rings and accelerators.

4. Use of the Ring for Electron and Stochastic Cooling

Stochastic cooling has been successfully tried out on the ISR and electron cooling has been tested in Budker's Laboratory. We, therefore, have strong evidence that the general principles behind these cooling techniques are correct. In detail, however, there is still a great deal to be learned about stochastic cooling and electron cooling, especially as it applies to the problem of collecting and cooling a large bite in $\bar{p}$ phase space in order to construct a $\bar{p}$ injector for Fermilab. It appears that the same cooling ring that is used to store and cool the $\bar{p}$'s could be used to study these cooling processes using the copious beams of protons available from secondary targets. We would therefore propose to construct the cooling ring at the earliest possible date and carry out detailed studies of the cooling phenomena. A practical fallout from the electron cooling study might be the measurement of the e^- capture cross sections for the production of energetic H atoms. Such atoms can be useful in the heating of plasmas.

The cooling ring is therefore to be constructed in a flexible way with a varible range of parameters that would allow a detailed study of three dimensional stochastic cooling and electron cooling.

5. Cooling of Betatron Oscillations

About ten years ago, Budker[1] proposed electron cooling as a way to increase the phase space density of antiprotons stored in a small storage ring. He pointed out that the cooling process could replace the synchrotron radiation damping of e^+, e^- storage rings and permit high luminosity $p\bar{p}$ colliding beams. About five years later, Van der Meer[2] in an unpublished note, pointed out the possibility of cooling the betatron motion in a storage ring with a wide band electronic feed-back loop based on the detection of the microscopic fluctuations of the position of the beam. Experimental evidence of successful electron cooling and of stochastic cooling have been recently reported at Novosibirsk[3] and at CERN[4]. Recently, Cline, McIntyre and Rubbia[5] have pointed out that the high energy rings at CERN and at FNAL could be transformed into a $p\bar{p}$ storage ring of about 600 GeV in the center of mass. Finally the projected Energy Doubler[6] at FNAL could give access to the fantastic energy of 2000 GeV in the center of mass.[7]

The present paper concentrates on a realistic scheme of producing $\bar{p}$'s with sufficient phase space density to reach luminosities in excess of 10^{30} $sec^{-1}cm^{-2}$ at 600 GeV in the center of mass. The main step is repetitive accumulation with no increase of total phase space. The antiproton yield in a realistic collecting channel increases sharply over the energy interval 1.5-4 GeV/c and this contrasts with the increase of electronic cooling times ($\sim \beta^3\gamma^5$) and the technological difficulties of a high energy, high current electron cooling beam (about 100amps dc at 750 keV). A comparatively simpler and faster accumulation scheme is proposed. It can operate at higher antiproton momenta and is based on betatron damping with a low signal (10 V) feed-back loop.

Accumulation can be repeated until about a few times 10^{10} particles are stored. At this point, the damping time becomes increasingly long and the main stack must be separated from the newly injected beam. A two-stage accumulation scheme is proposed to reach higher numbers of antiprotons. Final operations are required in order to adjust the beam parameters to the injection in a storage ring.

6. Production of Antiprotons

Antiprotons must be produced in a high density target bombarded by the proton beam. In order to achieve a reasonable yield, the antiproton channel collects negative particles produced around the forward direction (0° production angle). The main beam is then conveyed to a beam dump. The useful duration of the proton burst is about four times the revolution of the storage ring (4 x 600 ns = 2.4 μs). Some R.F. manipulations in the main accelerator may be required in order to achieve the largest possible number of protons in this time period.

The target is an iridium rod, 4.4 cm long. Following a calculation by Ranft[8] one gets an overall target efficiency of 1.3. The total energy lost in the target can be as large as 10^5 Joules at each pulse and it leads to an instantaneous evaporation. An automatic replacement device must be provided. Care must be taken that the radioactive debris are safely handled.

The beam transport after the target must collect the largest

Table 1

Parameters of the $\bar{p}$ Focusing Front End

Nominal $\bar{p}$ momentum		3.0 GeV/c
Maximum accepted angles		
(a) Vertical plane	θ_V	30×10^{-3} rad
(b) Horizontal plane	θ_H	30×10^{-3} rad
Parameters of first doublet: (Q_1, Q_2)		
-free distance to first lens		2.5 m
-gradient of first lens (Q_1)		690 Gauss/cm
-gradient of second lens (Q_2)		560 Gauss/cm
Useful half-apertures of each lens (Q_1, Q_2)		
(a) Vertical		120 mm
(b) Horizontal		280 mm
Values of the β function at the target location		
(a) Vertical plane	β_V^*	2.5 cm
(b) Horizontal plane	β_H^*	10 cm
Emittances of the accepted beam		
(a) Vertical plane		$22.5\ \pi\ 10^{-6}$ rad m
(b) Horizontal plane		$90\ \pi\ 10^{-6}$ rad m
Maximum accepted momentum spread	$\frac{\Delta p}{p} =$	2×10^{-2}
Target material and length	Iridium rod,	4.4 cm
Target efficiency	η_T	0.33

Table 2

List of Parameters of First Doublet

Maximum field gradient	690 Gauss/cm
Current	1130 A
Voltage	145 V
Resistance at 50 C°	0.13 Ohm
Power consumption	162 KW
Magnetic length	1100 mm
Weight of copper	1.15 t
Weight of iron	10 t

possible fraction of $\bar{p}$'s produced. We have conisderd only standard quadrupoles, i.e., we have excluded the use of pulsed lenses and/or sup and/or superconducting elements. A possible design is shown in Fig. 2. The main parameters of the critical front end of the $\bar{p}$ focusing channel are listed in Table 1. The first qudrupole doublet of lenses is taken from a realistic design (the storage ring DORIS). Parameters are given in Table 2. A drawing of the lens is shown in Fig. 3. In order to accommodate the required emittances, the aperture must be as large as 52 x 24 cm^2. Subsequent lenses are necessary to match the $\bar{p}$ beam to the betatron functions of the ring. Bending magnets move the residual proton beam to a beam dump and match momentum compactions. The whole beam transport is pulsed only for a short period during each injection cycle.

The yield of antiprotons produced in the momentum interval $3 < p < 4$ GeV/c and in the forward direction for an incident proton energy $E_p = 23.1$ GeV on a lead target has been measured by Dekkers et al.[9]:

$$\frac{d^2N}{dpd\Omega} = 2 \times 10^{-2}\ \mathrm{GeV}^{-1}\mathrm{st}^{-1}(\mathrm{int.}\ p)^{-1}.$$

Since the acceptance of the injection channel is relatively large, the variation of yield with the angle of production must be taken into account. The following parameterization has been assumed for the invariant cross section:

$$E\frac{d^3N}{dp^3} = e^{-6p_\perp} f(p_{||}).$$

Integration up to an angle of θ_M from the forward direction gives

$$\frac{dN}{dp} = 1.93 \times 10^{-4}(1 - e^{-6p\theta_M})\ \text{GeV}^{-1}(\text{int. p})^{-1}$$

The fraction of the accepted $\bar{p}$'s as a function of θ_M is displayed in Fig. 4. For $\theta_M = 30 \times 10^{-3}$ rad., about 40% of $\bar{p}$'s are collected and $\frac{dN}{dp} = 7.72 \times 10^{-5}$ $\text{GeV}^{-1}(\text{int. p})^{-1}$. Assuming $\frac{\Delta p}{p} = 2.0 \times 10^{-2}$, i.e., $\Delta p = 60$ MeV/c, we get $N_{\bar{p}} = 4.63 \times 10^{-6}(\text{int. p})^{-1}$ (at $E_p = 23.1$ GeV). Including target efficiency (1/3) and the corrections due to the finite target length (0.9), we arrive at the figure: $N_{\bar{p}} = 1.53 \times 10^{-6}$ $(\text{incident p})^{-1}$ (at $E_p = 23.1$ GeV). For incident protons of $E_p \geq 60$ GeV, we assume a yield 2.5 times larger, i.e., $N_{\bar{p}} = 3.84 \times 10^{-6}$ $(\text{incident p})^{-1}$.

The FNAL accelerator, at the time of the proposed experiment, probably will have reached the design intensity of 5×10^{13} ppp. One turn ejection will then give 6.36×10^{12} protons over the 4 turns of the storage ring. We can hope to accumulate about 2.44×10^{7} $\bar{p}$'s at each injection pulse. This is only 10% of the available protons from the accelerator. Schemes are possible, in which bunching at low frequency is used to increase considerably the useful number of antiprotons. We shall not consider these improvements at the present stage.

7. The Storage Ring

The main features of the lattice of the storage ring can be reasonably well defined by simple considerations. The first choice is the momentum of the antiprotons, which has been somewhat arbitrarily set to 3.8 GeV/c as a compromise between size, cost and performance. This, in turn, leads to two possible choices of the

Table 3

Main Parameters of the Cooling Ring

I. Lattice and Orbit Parameters

- Nominal momentum	p_o	3.8 GeV/c
- Guide field	B_o	12.0 K Gauss
- Curvature radius (magnetic)	ρ	10.66
- Average radius	R	34.8 m
- Number of periods	N	16
- Period structure		0/2 BBDFDBB0/2
- Period length	ℓ_p	16.54 m
- Number of bending magnets/period		4
- Quadrupole gradient for $\nu = 1.75$	F	690 G/cm
	D	480 G/cm
- Quadrupole gradient for $\nu = 2.25$	F	157 G/cm
	D	157 G/cm
- Nominal length of F-quadrupole		0.75 m
- Nominal length of D-quadrupole		0.5 m
- Nominal length of bending magnet		2.09 m
- Length of interelement gap		1.0 m
- Free length in empty semi-period		8.0 m
- Nominal working point	$\nu\begin{Bmatrix}\nu_x = 1.84\\ \nu_y = 1.68\end{Bmatrix}^*$	= 2.25
- Total transistion energy/rest energy	γ_t	1.9
- Phase advance/period	μ	81°
- Maximum β value in F-quadrupole	$\hat{\beta}_H$	22.97 m
- Minimum β value in F-quadrupole	$\check{\beta}_V$	9.45 m
- Maximum β value in D-quadrupole	$\hat{\beta}_V$	14.88 m
- Minimum β value in D-quadrupole	$\check{\beta}_H$	8.78 m

Table 3 (cont.)

- Maximum of momentum compaction function	$\hat{\alpha}_p$	8.78 m
- Minimum of momentum compaction function	$\check{\alpha}_p$	5.65 m

*Basic structure - long straight section at 1 integer each $2\nu_x$ and 1/2 integer each 2 ν_y, thus ν_x = 5.84 and ν_j = 3.68 for this machine with 4 long straight sections.

II. Dipole Magnets

- Number of units	32
- Nominal length	2.09 m
- Gap height	100 mm
- Useful width	225 mm
- Lamination height	50.8 cm
- Lamination width	155 cm
- Core weight (packing fraction 0.96)	13.4 tons
- Copper weight	2.0 tons
- Number of turns	120
- Conductor dimension	43 x 14.25 mm^2
- Cooling hole	6 m dia
- Ampere turns	100,000
- Nominal current	850 A
- Current density	500 amp/sq in
- Power losses	18 KW
- Resistance	7.2 x 10^{-3} Ohm
- Voltage drop/unit	11.4 volts

Table 3 (cont.)

III. Quadrupole Lenses	
- Number of units	20
- Field gradient	250 Gauss/cm
- Current	285 A
- Voltage	7.5 V
- Power consumption	2.13 KW
- Magnetic length	590 mm
- Number of turns/coil	25
- Conductor dimensions	11 x 11 mm^2
- Cooling hole (ϕ)	4 mm
- Iron weight	820 Kg
- Copper weight	140 Kg
IV. Main Power Supply	
- Bending magnets	
(a) Voltage	250 V
(b) Current	1580 A
- Quadrupole lenses (2 separate supplies for D and F)	
(a) Voltage (each supply)	82 V
(b) Current	285
- Total installed power for magnets	500 KW

Table 3 (cont.)

V. Correcting Elements	
- Sextupoles	16
- Octupoles	16
- Bending magnets for orbit correction	32
- Skew Quadrupoles (45°-tilt)	2
- Pick-up stations (for R.F. bunched beam only)	40
VI. Vacuum System	
- Ring average pressure (90% H_2, 10% N_2)	10^{-10} Torr
- Number of ion pumps	40
- Number of rotary pumps	5
- Chamber wall thickness	2 mm
- Bake-out heating elements and thermal insulation thickness	7 mm
- Temperature of bake-out	350C°
- Inner vacuum chamber apertures	
(a) Vertical	80 mm
(b) Horizontal	225 mm

transition energy γ_t (in units of the rest mass) which must be kept as far as possible from the working point: $\gamma_t >> 3$ and (b) $\gamma_t << 3$. Alternative (b) is preferred because stochastic damping requires the largest possible randomizing effect from the momentum spread.

Another relevant consideration is the radial aperture associated with the momentum spread of the beam at injection. The average radial displacement $<\Delta r>$ around the orbit and the fractional momentum error $\frac{\Delta p}{p}$ are related by the average value of the momentum compaction function $<\alpha p>$:

$$<\Delta r> = <\alpha p>\frac{\Delta p}{p}$$

The transition energy in turn is connected to $<\alpha p>$ by the relation:

$$\gamma_t = \sqrt{R/<\alpha p>}$$

where R is the average radius of the ring. A reasonable choice is $<\alpha_p> \simeq 4$ m, corresponding to a radial aperture allowance of 8 cm for $\Delta p/p = 2\%$. Since $R \simeq 2\rho = 32$ m, $\gamma_t \cong 2.00$. Furthermore, we can relate γ_t to ν the number of betatron oscillations/turn because of the relatively exact expression $\gamma_t \simeq \nu$. Taking ν values equally distant from integer and half integer resonances gives quantized values of $\nu = 1.25, 1.75, 2.25, 2.75$ and so on. The value $\nu = 2.25$ is the one suggested by the previous considerations. The number N of equal cells around the circumference of the ring is related to ν by the betatron phase advance/cell, $\mu = \nu/2\pi N$. For optimized designs, the phase advance has a value approximately around $\pi/2$, giving $5 < N < 15$. Lower values of N are preferable since (a) we can get the largest straight sections for given values of R and ρ and (b) we can exploit the characteristic shape modulation of the size due to the strong focusing in order to optimize the apertures of the components around the ring. Several possible alternatives of the initial parameters have been considered.

The main parameters of an example ring are given in Table 3. A schematic drawing of the ring is shown in Fig. 1a. A possible magnet and vacuum chamber design is shown in Fig. 1b.

8. Injection and accumulation

The injection is performed in four turns in order to collect the longest possible proton burst from the accelerator (Fig. 4b). Since the diameter of the ring is ~200m, this corresponds to an injection time of 2.4 μs. Injection of the new beam must not disturb the main stack already present in the ring. The vertical plane is preferred since in this way the stochastic damping is not affected by radial effects due to momentum spread. The injection procedure is as follows:

(i) a pair of fast (~50 ns risetime) kickers produce a vertical bump of few centimeters in order to bring the injection septum within the aperture of the ring. The bump however leaves enough aperture around the equilibrium orbit, so that the main stored beam does not hit the septum. (See Fig. 5)

(ii) The new beam is injected through the septum and four turns are stored before the first injected particle reaches the septum. At this moment the bump is quickly turned off (~50 ns decay time) and the injected beam appears in the phase space diagram as a halo around the old stack (Fig. 6).

(iii) After a few milliseconds to let π^-, K^-, etc. decay, the betatron cooling is turned on and it collapses the newly injected beam on the old stack (Fig. 7a,b,c,d,e). Note that the old stack is continuously damped, thus correcting the inevitable phase space blow-up due to the injection procedure.

The stochastic damping parameters[10] are summarized in Table 4. Figure 8 shows the expected stacking time as a function of the number of antiprotons present in the ring. Note that the large momentum spread is necessary in order to randomize the sample in a few turns.[2] If C is the circumference of the orbit,

$$\frac{\Delta C}{C} = \left(\frac{1}{\gamma^2} - \frac{1}{\gamma_t^2}\right) \cdot \frac{\Delta p}{p} .$$

For C = 200m, $\frac{\Delta p}{p} = 10^{-2}$, $\gamma_t = 2.0$, and $\gamma = 3.6$,

we get $\Delta C = 0.35$ m/revolution, which is just adequate.
If, for instance, instead $\frac{\Delta p}{p} \sim 10^{-3}$, according to Monte Carlo simulations we expect an increase of about 7 times in the cooling time.

The horizontal betatron motion is almost certainly weakly coupled with the vertical one by the presence of parasitic fields. It is therefore advisable to damp both modes of oscillations. This can be done very simply by increasing the coupling of the two modes with a skew quadrupole.

9. Damping of momentum spread

After a few times 10^{10} particles are accumulated in the ring, the stacking time becomes quite long and it is advisable to remove the main beam. At this point we propose to reduce the momentum spread with stochastic momentum damping. The main parameters of the momentum damping[10] are listed in Table 5. The main feature of momentum damping is that its rate becomes progressively slower as

Table 4

Main Parameters of Betatron Stochastic Damping

Pickup aperture		30 cm
Pickup length		50 cm
Pickup bandwidth		from 100 MHz to 400 MHz
Equivalent sample length		50 cm
Noise figure of amplifier		3 db
Pickup importance		120 ohm
Number of pickup elements		16
Deflector		
Deflector length (code unit)		50 cm
Number of units		4
Deflector aperture		30 cm
Deflecting power		4.75×10^{-8} rad/volt
Cooling parameters at	2.5×10^{7} $\bar{p}$	2.5×10^{10} $\bar{p}$
Antiproton current	6.6 μA	6.6 mA
Number of $\bar{p}$'s in sample	1.4×10^{4}	1.4×10^{7}
R.M.S. rise at end cooling cycle	1.0 cm	1.0 cm
R.M.S. fluctuation in average position	84 μ	2.67 μ
R.M.S. signal from 16 pickups	59.1 mA	1.87 μA
R.M.S. noise from 16 pickups	565 nA	565 nA
Cooling time at optimum gain	11.4 sec	12.5 sec
R.M.S. deflection angle (at optimum gain)	5.74×10^{-8} rad	1.66×10^{-7} rad
Total R.M.S. voltage	11.55 V	3.49 V

Table 5

Parameters of the Momentum Cooling

Pickup aperture		30 cm
Pickup length		75 cm
Pickup bandwidth		from 100 to 200 MHz
Sample length		1.5 m
Number of pickup elements		16
R.F. cavities		10
R.F. cooling impedance		100 Ω
Cooling parameters at		2.5×10^{10} $\bar{p}$
Number of $\bar{p}$ in sample		4.2×10^{7}
R.M.S. momentum spread		
(a) at beginning	0.84×10^{-2}	
(b) at end cooling		0.84×10^{-3}
R.M.S. fluctuation of energy	3200	320 eV
R.M.S. signal from pickup	7.56	0.745 μA
R.M.S. noise from 16 pickups	565 nA	565 nA
Cooling time (inverse rate) of optimum gain	(335) 187 sec	1300 sec
R.M.S. voltage in each cooling	(184 V) 220 V	32 V
Power in each cavity	(340 V) 84 kV	84 W
Beam invariant area	36 eV sec	3.6 eV/sec

$\frac{\Delta p}{p}$ diminishes because of the corresponding increase of the de-randomizing time of the sample.[2] It is impractical to reduce the momentum spread to less than about $\frac{\Delta p}{p}$ ~2×10^{-3} full width. This corresponds to an invariant phase area of the beam of 3.6 eV sec, which is still much too large to be injected in the main ring. We propose at this point to capture adiabatically the beam with R.F. of the lowest harmonic number (h=1) and to decelerate it until it reaches approximately 350 MeV/c, corresponding to about 60 MeV kinetic energy. The relative beam sizes will increase by the factor $(\beta\gamma)^{1/2}$ which is about 3.16. The available apertures should then be sufficient. The momentum spread will also increase to about 7×10^{-3} after adiabatic debunching. Assuming some blow-up in the debunching process, it is probably appropriate to assume that the beam will have a forward relative momentum spread $\frac{\Delta p}{p} = 10^{-2}$ at p = 350 MeV/c.

The minimum R.F. voltage required to capture at p = 3.0 GeV/c a beam of area A = 4 eV-sec and h = 1 is easily calculated. It is

$$V_o = 7280 \text{ Volt} \qquad \text{at } f_o = 1.7 \text{ MHZ}.$$

At the value p = 350 MeV, these figures change to:

$$V_o = 1748 \text{ Volt} \qquad \text{at } f_o = 580 \text{ KHZ}.$$

One simple cavity of the type PPA (drift tube) is amply sufficient in order to provide the required voltage.

10. Brief Summary of the Theory of Electron Cooling

The Novosibirsk group has demonstrated that low momentum proton beams can be "cooled" to very small transverse dimensions ($<1mm^2$) and very small momentum spread ($<\delta p/p < 10^{-4}$). The basic idea is that the transverse and longitudinal oscillations of the proton beam are transferred to an electron beam that is injected in one of the straight sections of the storage ring. For maximum cooling efficiency the velocity of the $\bar{p}$ and of the e^- should be the same ($\beta_{\bar{p}} = \beta_{e^-}$) since the coulomb scattering cross section will be a maximum.

The cooling time for a parallel e^- and p (or $\bar{p}$) beam is given by ($\delta\theta_e << \delta\theta_{\bar{p}}$)

$$\tau = 0.5 \left(\frac{M_{\bar{p}}}{m_{e^-}}\right) \frac{\gamma_{\bar{p}}^5 \beta_{\bar{p}}^3 (\delta\theta_{\bar{p}})^3}{n_e r_e^2 cL\, \eta\, \ell n\, (\delta\theta_{\bar{p}}/\delta\theta_e)}$$

where r_e = classical electron radius

n_e = electron beam density

$\delta\theta_{\bar{p}}$ = $\bar{p}$ beam divergence

$\gamma = E_{\bar{p}}/m_{\bar{p}}$, $\beta_{\bar{p}} = (P_{\bar{p}}/E_{\bar{p}})$

η = cooling length/total circumference of cooling ring

L = cooling length (M)

The important features of the cooling time formula is

$$\tau \propto \frac{1}{(\text{cooling length})} \frac{\gamma_{\bar{p}}^5\ \beta_{\bar{p}}^3\ (\bar{p}\text{ beam Divergence})^3}{[n_e]}$$

The γ^5 factor increases the cooling times, for reasonable electron current densities, to very long times at high $\bar{p}$ moments. [i.e., ($\bar{P}_p$ = 3 GeV/c), $\gamma^5 \simeq 243$]

The dependence on the $\bar{p}$ beam divergence shows the desirability of precooling the $\bar{p}$ beam to reduce the divergence. Finally, the cooling time depends inversely on the cooling length and electron beam density. It is clear that the γ^5 and $(\text{divergence})^3$ factors dominate the cooling time and since the cooling length and electron current are linear efforts, electron cooling must be carried out at low momenta.

11. Electron Cooling Times

At 350 MeV/c $\bar{p}$ momenta very short cooling times can be achieved with rather modest electron beams. A schematic of the cooling straight section is shown in Fig. 9. Electrons are obtained from a large aperature electron gun (Pierce gun) accelerated to a 33 KeV and injected into the storage ring. The electron beam divergence is kept low with a small longitudinal magnetic field in the storage ring. The electrons are deflected out of the storage ring, and deaccelerated and collected in a Faraday cup. The power dissipation is kept low by good electron beam optics. An inefficiency of $\sim$1% seems possible. The expected cooling times are given in Table 6 along with the current density and expected power dissipation. Note that the cooling times are quite short even for modest electron currents and resulting small power dissipation. The electron guns and power supply needed for the electron cooling are modest and easily obtained commercially.

We expect that the electron cooling will reduce the transverse dimension of the $\bar{p}$ beam to $\leq 1\ \text{mm}^2$ and the beam momentum spread $< 10^{-4}$. The exact values depend on the residual gas scattering and the accuracy of satisfying the velocity conditions $\beta_{\bar{p}} = \beta_{e^-}$.

12. Luminosity Estimates

In order to estimate the luminosity we parameterize the lumi-

Table 6

Electron Cooling Times (350 MeV/c $\bar{p}$'s)

(5m Cooling Length)

Beam Size	e^- Current/cm^2	Cooling Time	Power Dissipation (1% Off)
1 cm^2	0.1 amp/cm^2	30 sec	0.16 KW
10 cm^2	1 amp/cm^2	3 sec	15 KW
10 cm^2	0.1 amp/cm^2	30 sec	1.5 KW

nosity as a function of the number of protons and antiprotons in the machine. Figure 10 shows the resulting isoluminosity curves. The assumed emittance for the proton and antiproton beam is also given on Fig. 10.

13. Costs, Early Tests and Time Table

We have estimated the cost of the cooling ring and associated devices. The estimates are listed in Table 7. These numbers are extrapolations from previous projects known to us. Harder numbers will be available by mid summer 1976 as a more complete cooling ring design is obtained.

The early tests of the cooling ring beyond simply making it work will concentrate on the study of stochastic and electron cooling of proton beams. We note that cooled proton beams might be useful to decrease the emittance of the protons in the main ring and increase the luminosity of the $\bar{p}p$ colliding beam devices. Independent of this possibility we wish to study the parameters of stochastic and electron cooling to better understand these phenomena. After the proton cooling studies we would start injecting antiprotons to study the accumulation times and characteristic cooling times as well as R. F. bunching. Finally the deacceleration of the antiprotons would be attempted and the electron cooling option.

Table 7

Estimated Cost of Cooling Ring

	$\times 10^6$ \$
Design	0.1
Electron Cooling	0.5
Stochastic Cooling	(0.5 - 1)
Dipoles	0.5
Quadrupoles	0.16
Vacuum Chamber	1.2
Power Supply	0.5
R. F. System	0.5
Injection	0.75
Extraction	0.25
	4.96 (5.46) $\times 10^6$ \$

In order to study the injection of antiprotons into the main ring we suggest that protons be used initially and accelerated the wrong direction in the main ring. We realize that the scheme of collecting, storing, cooling and reinjection protons or antiprotons into the main ring is very complex, however, we remind the reader that the scheme for obtaining 5×10^{13} protons per pulse in the present Fermilab machine seemed extremely complex only 5 years ago, but now is taken for granted.

The tentative time table for the cooling ring is as follows:

August 1976	CP and D funding starts (??)
September 1976	Full Ring design
October 1976	First prototype dipole and quadrupole magnet construction and field map
January 1977	Bids out for dipole and quadrupole magnets and coil construction
(Allow 8 months for magnet construction)	
Summer 1977	Start vacuum chamber and ion pump construction - R. F. prototype
Fall 1977	Prototype stochastic and Electron cooling devices
January 1978	Start assembly of cooling ring at Fermilab
Spring 1978	Install R. F. system
Summer 1978	Install electron cooling and stochastic cooling devices
Fall 1978	Install beam injection and extraction system
Fall 1978	First injection of protons and antiproton and study of cooling phenomena

January 1979	First injection of antiprotons into Fermilab main ring
Spring 1979	Complete detector at interaction region
Summer 1979	Start of $\bar{p}p$ colliding beam experiments
Fall 1979	Observe first W production

14. Comments

It is expected that other people will join this effort including Rae Steining and perhaps others from Fermilab.

We wish to thank all the people who have patiently explained some of the details of cooling to us and have critizied our thinking on this subject.

We would like to especially acknowledge Drs. T. Collins, R. Herb, F. Halzen, S. Glashow, E. Picasso, G. Petrucci, N. Ramsey, L. Sulak, L. Thorndahl, L. Teng and S. Weinberg for helpful discussions and suggestions.

REFERENCES

1. G. I. Budker, Atomic Energy 22, 346 (1967).

2. S. Van der Meer, CERN-ISR-PS/72-31, Aug. 1972 (unpublished).

3. G. I. Budker, Y. S. Derbenov, N. S. Didonsky, V. I. Kudelainen, I. N. Meshkov, V. V. Perkhomduk, D. V. Pestrikov, B. N. Sukhine, A. N. Shrinkskig, Experiments on Electron Cooling, paper presented at the National Conference, Washington, March, 1975.

4. P. Braham et al., NIM 425, 156 (1975).

5. C. Rubbia, P. McIntyre and D. Cline, Producing the Massive Intermediate Vector Meson with Existing Accelerators, submitted to Phys. Rev. Letters, March, 1976.

6. Proposal for the Energy Doubler (1975).

7. D. Cline and C. Rubbia, Energy Doubler at FNAL as a High Luminosity $p\bar{p}$ Storage Ring Facility. Report in preparation.

8. J. Ranft: CERN Computer Library Program and Karl Marx University Preprint, Leipzig KMU-HEP-7412 (1975).

9. Dekker et al., Phys. Rev. 137, C962 (1965).

10. For a complete description of relevant formulae see L. Thorndahl, CERN-ISR-RF 75-(Closed Distribution), December 1975.

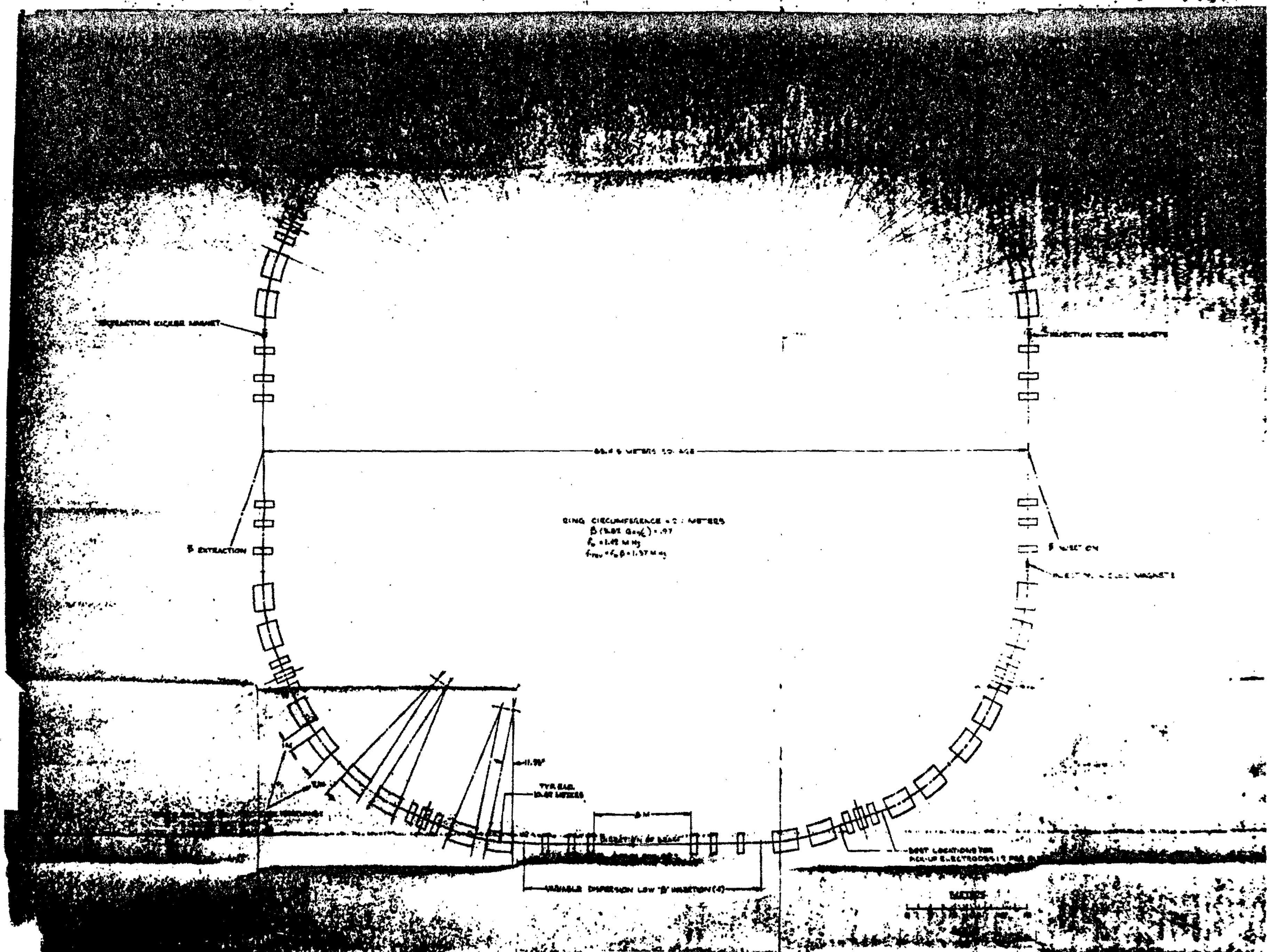

Fig. 1a

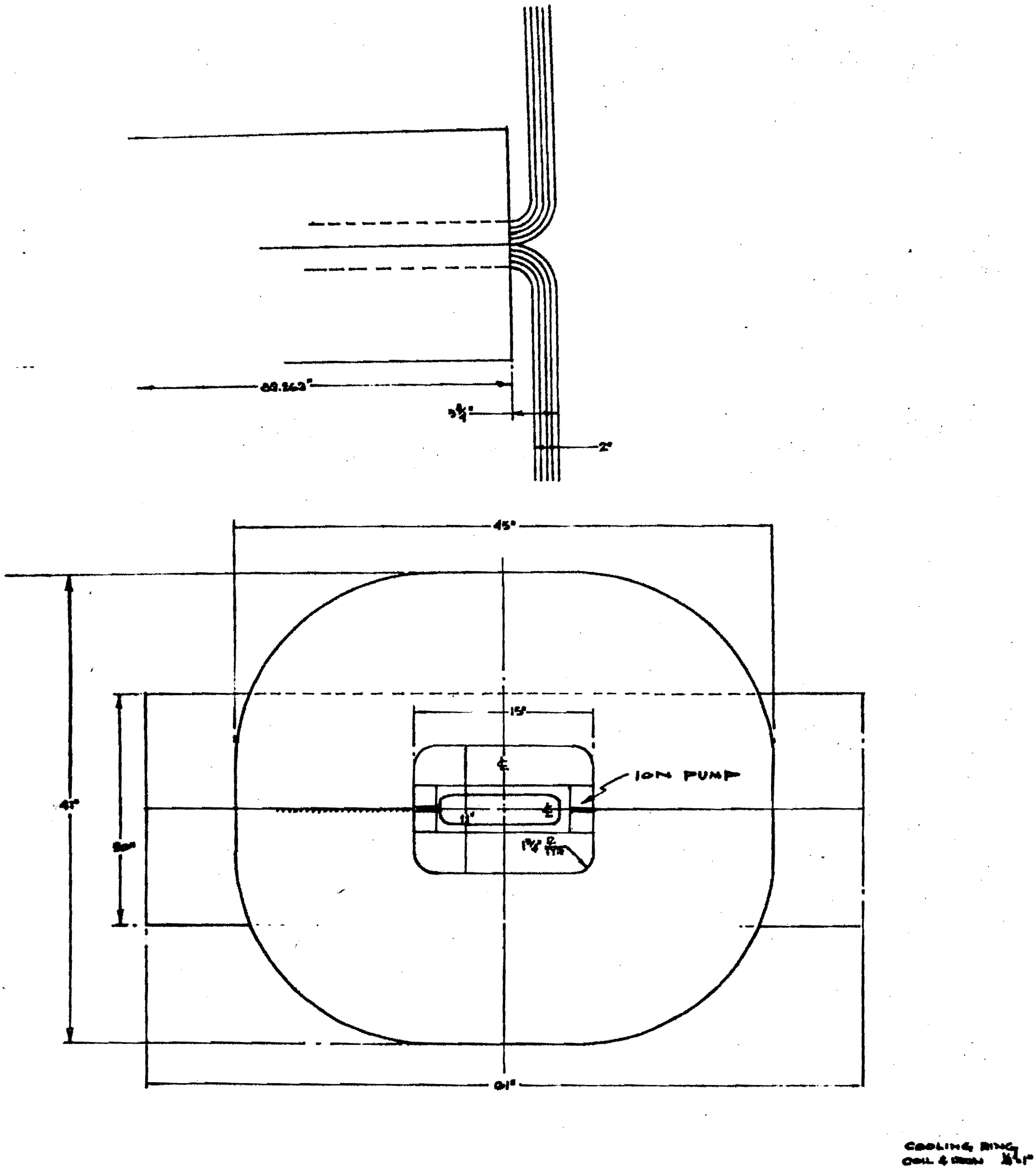

Fig. 1b

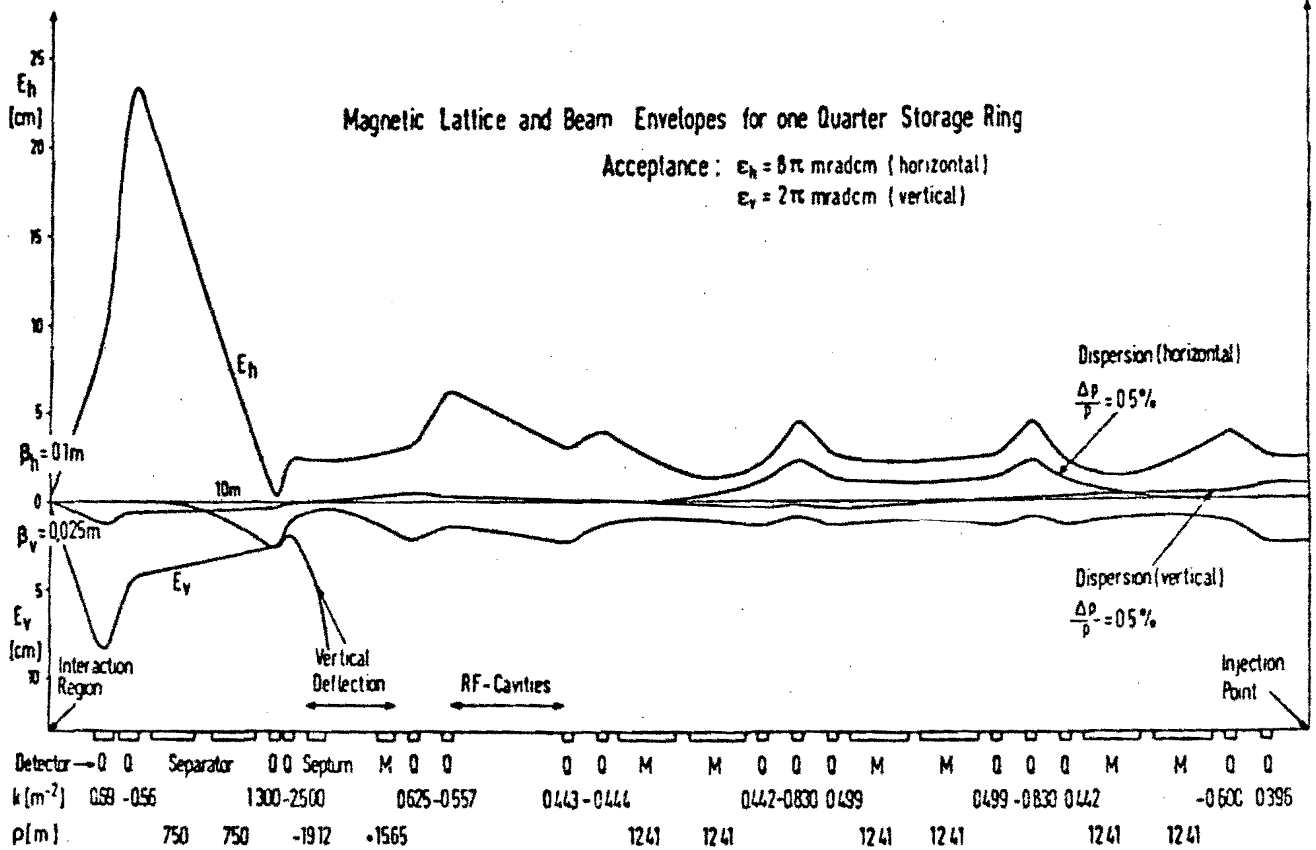

Magnet lattice, beam envelopes and dispersions for one quarter storage ring (ϵ_h = 8mrad·cm, ϵ_v = 2mrad·cm, $\frac{\Delta p}{p_o}$ = 0,5%)

Fig. 2a

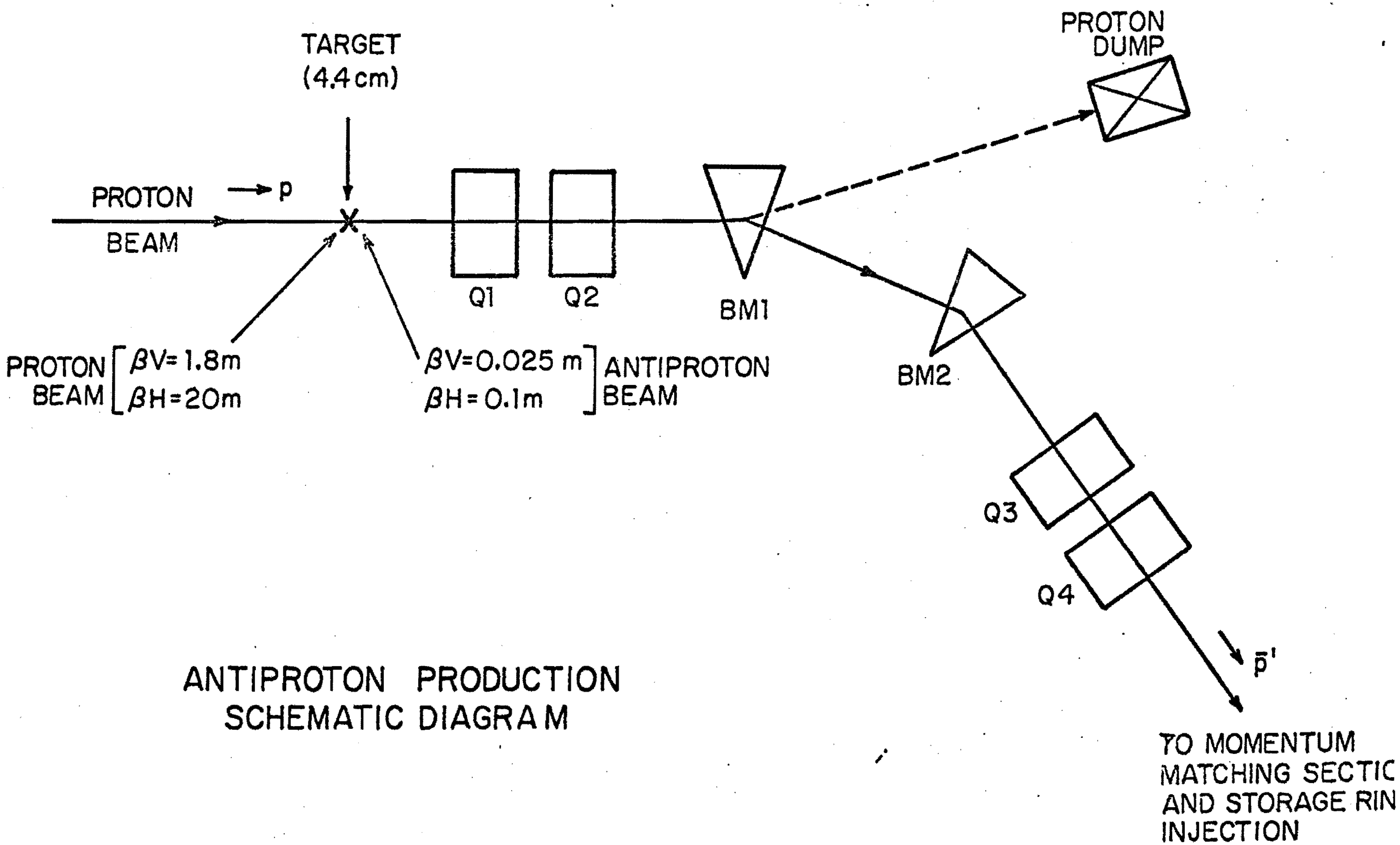

TARGET
(4.4 cm)
PROTON
DUMP
PROTON
BEAM
→ p
Q1
Q2
BM1
BM2
PROTON
BEAM
βV= 1.8m
βH=20m
βV=0.025 m
βH=0.1m
ANTIPROTON
BEAM
Q3
Q4
p̄'
TO MOMENTUM
MATCHING SECTIC
AND STORAGE RIN
INJECTION
ANTIPROTON PRODUCTION
SCHEMATIC DIAGRAM

Fig. 2b.

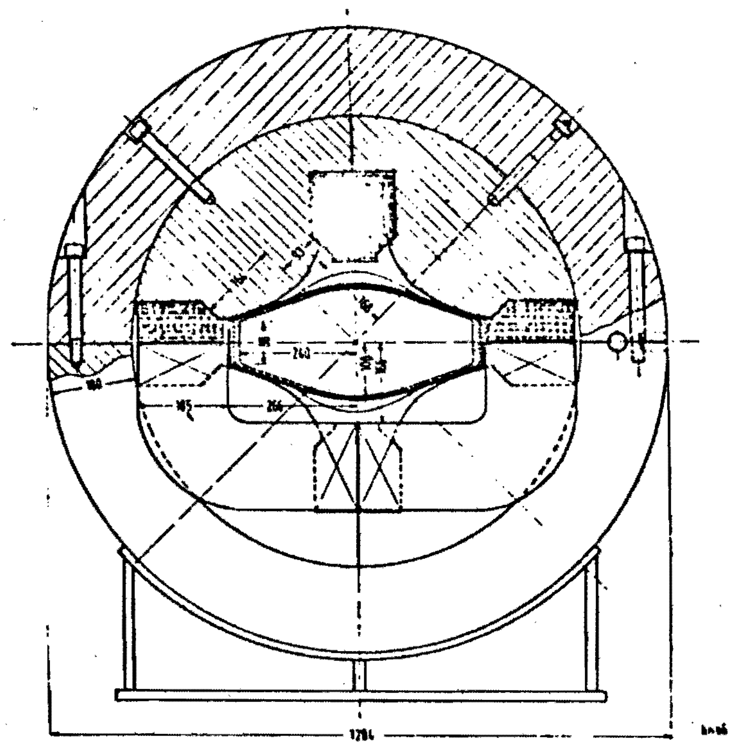

Fig. 3

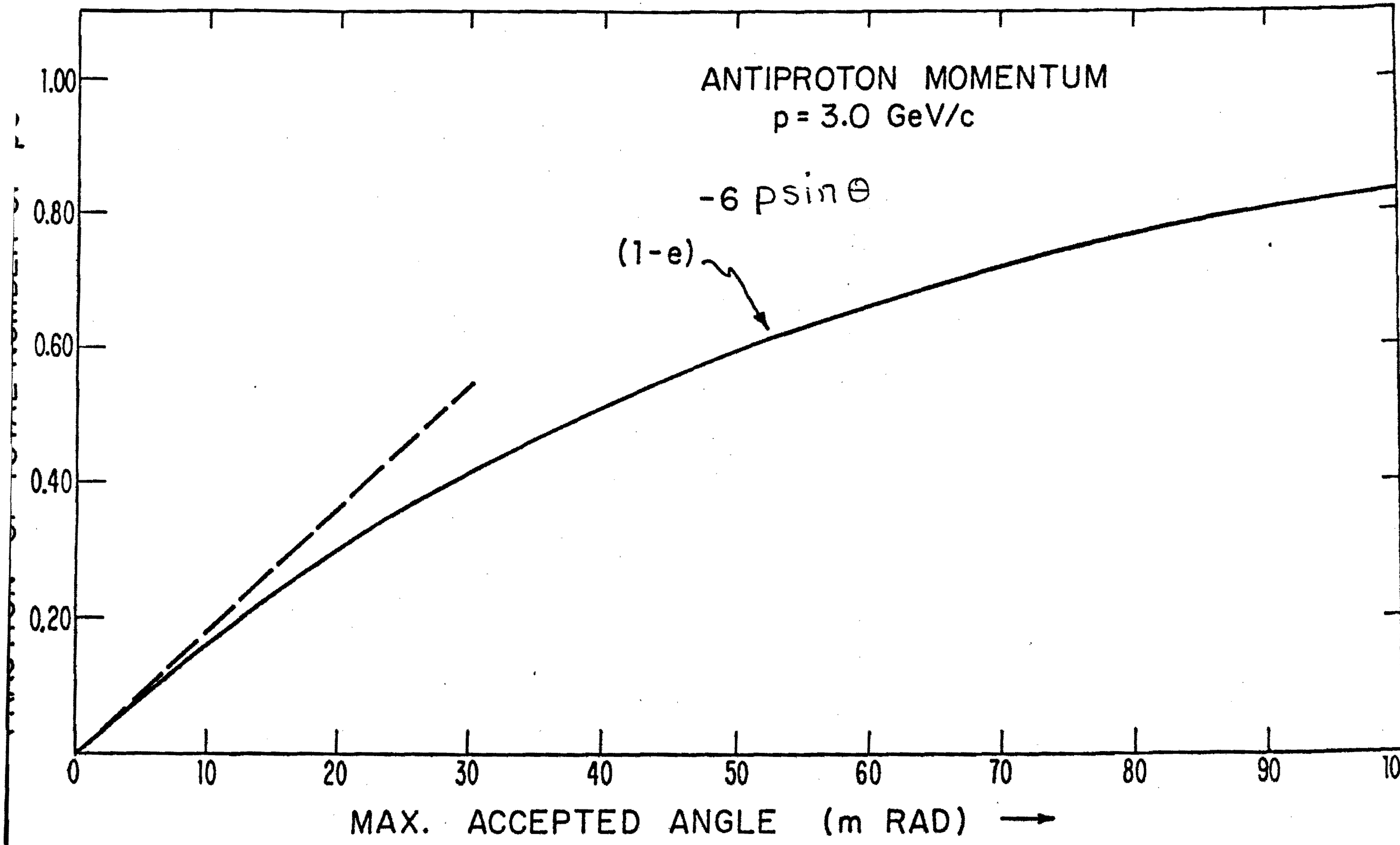
ANTIPROTON MOMENTUM
p = 3.0 GeV/c
-6 psin θ
(1-e)
1.00
0.80
0.60
0.40
0.20
0
10
20
30
40
50
60
70
80
90
100
MAX. ACCEPTED ANGLE (m RAD)

Fig. 4

FOUR TURN INJECTION SCHEME IN VERTICAL PLANE

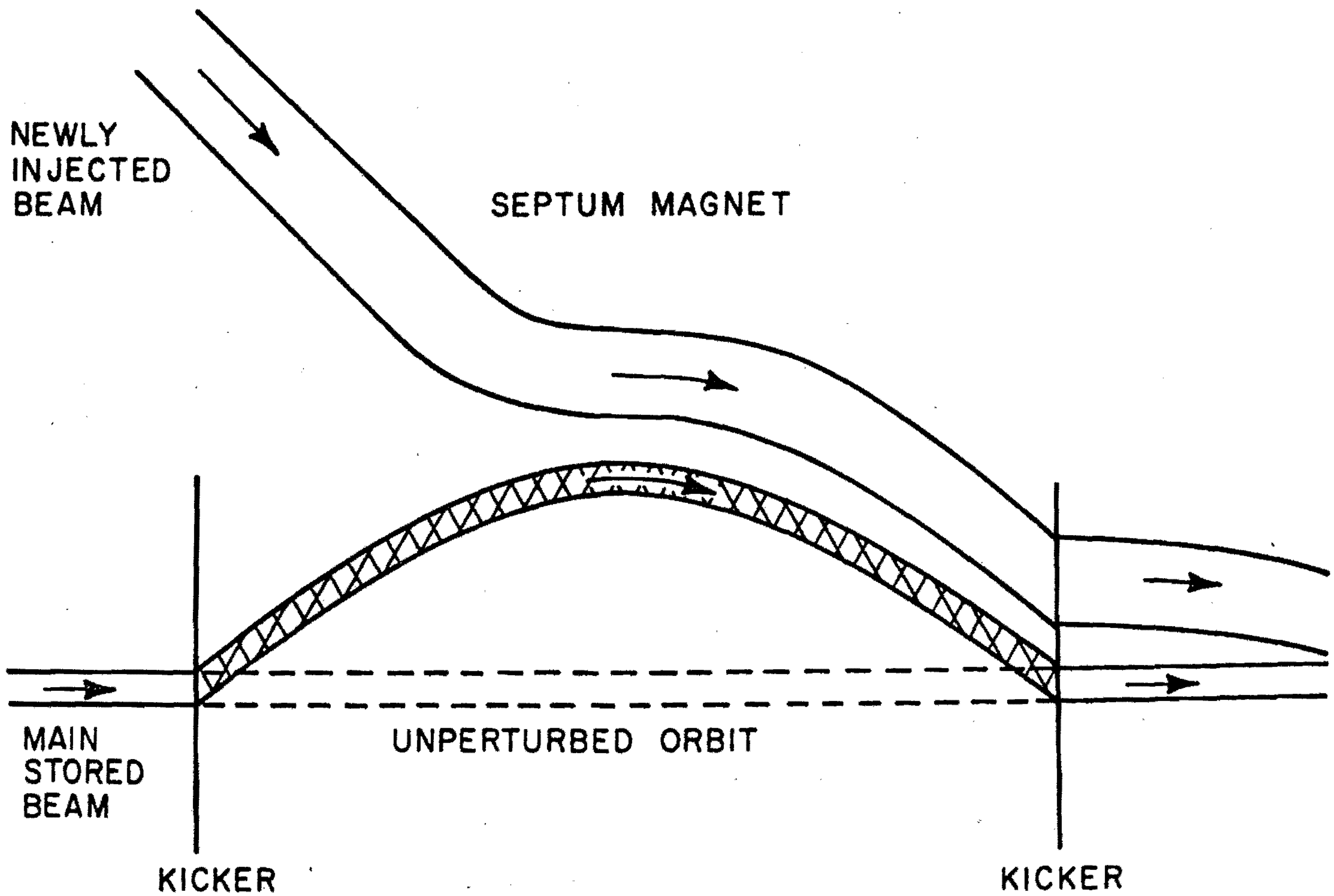

Fig 5

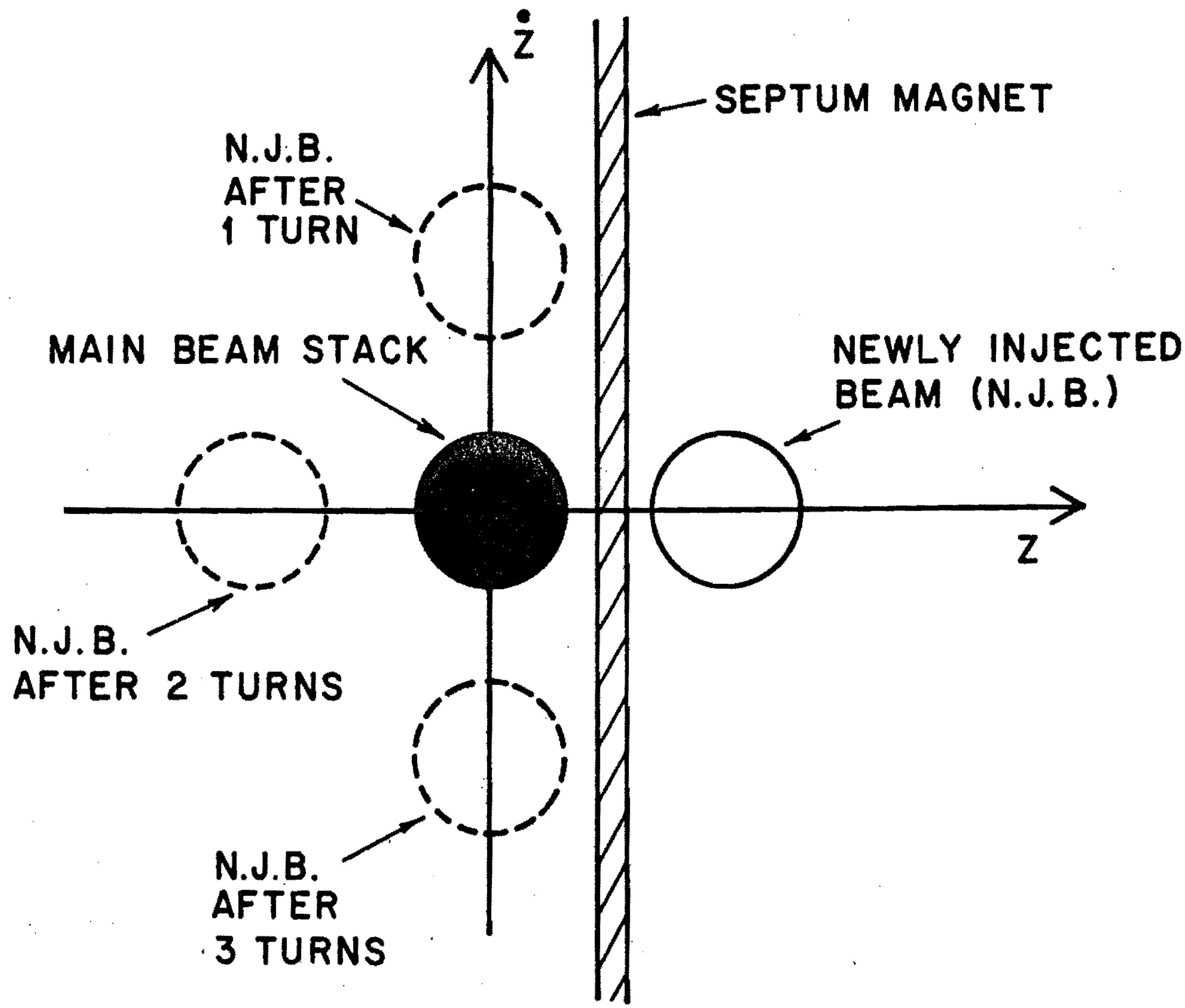

Ż
SEPTUM MAGNET
N.J.B.
AFTER
1 TURN
MAIN BEAM STACK
NEWLY INJECTED
BEAM (N.J.B.)
Z
N.J.B.
AFTER 2 TURNS
N.J.B.
AFTER
3 TURNS

Fig 6

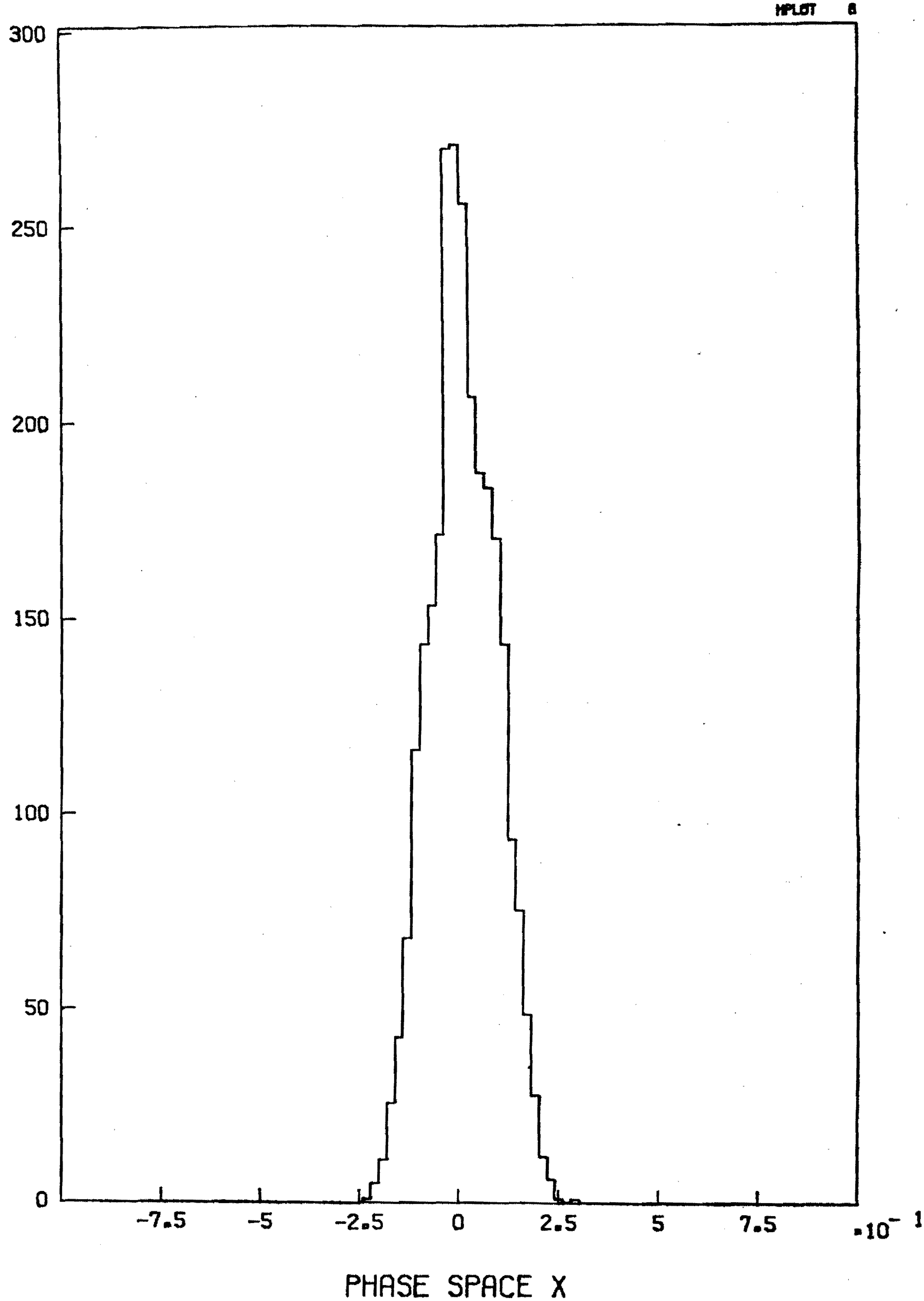

Fig. 7a

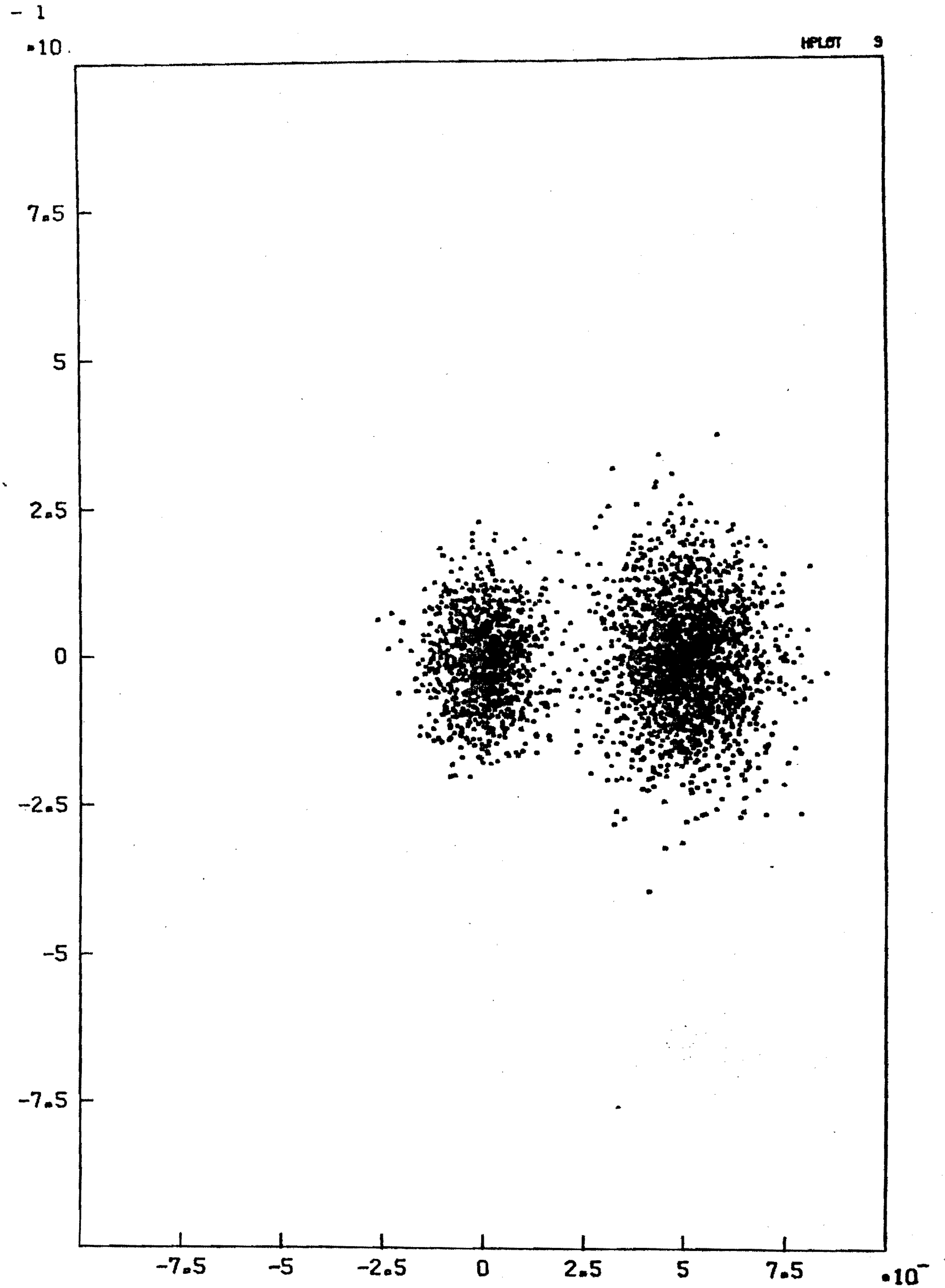

INITIAL PHASESP. Y

Fig. 7b

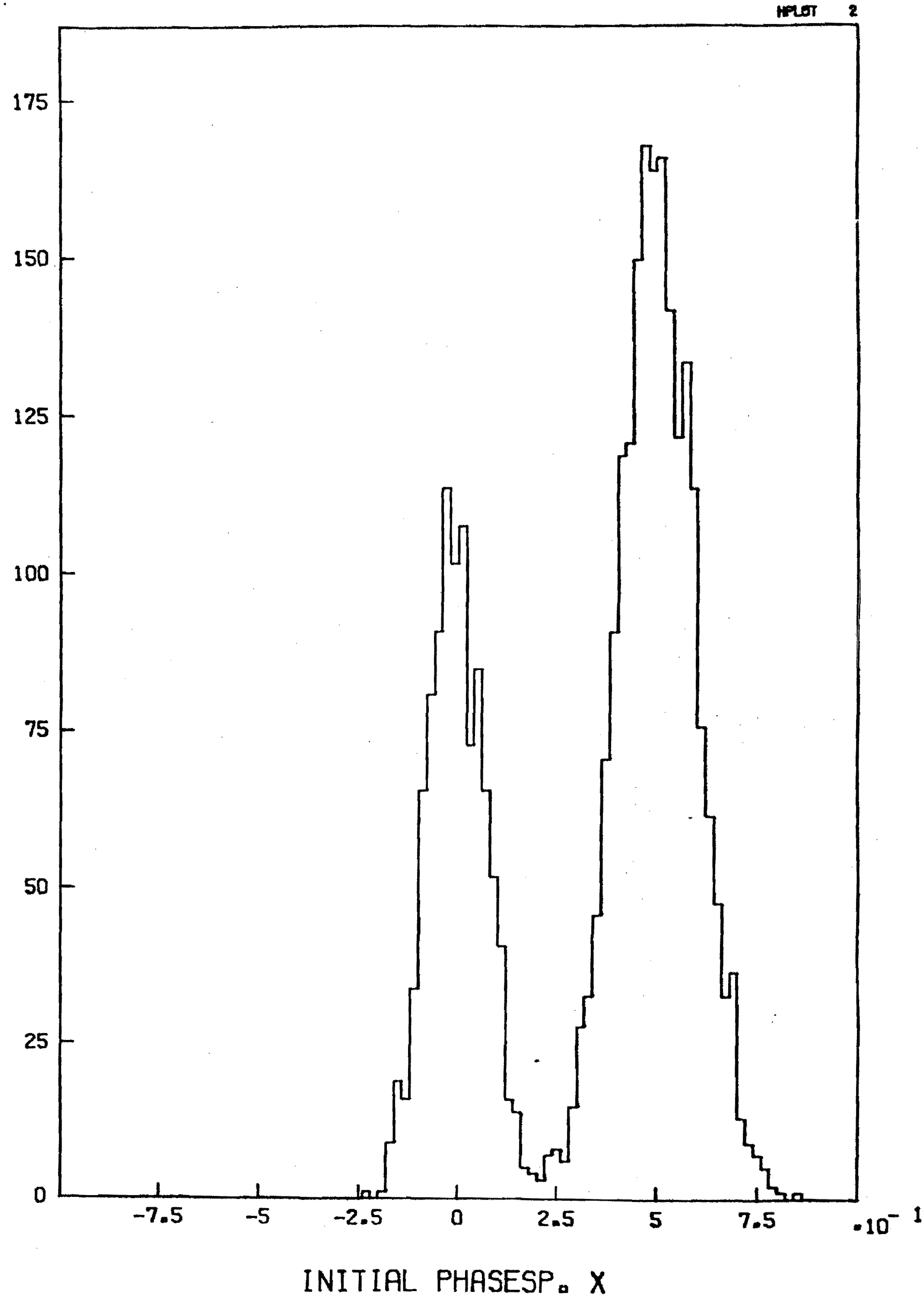
HPLOT 2
175
150
125
100
75
50
25
0
-7.5
-5
-2.5
0
2.5
5
7.5
*10⁻ 1
INITIAL PHASESP. X

Fig. 7b

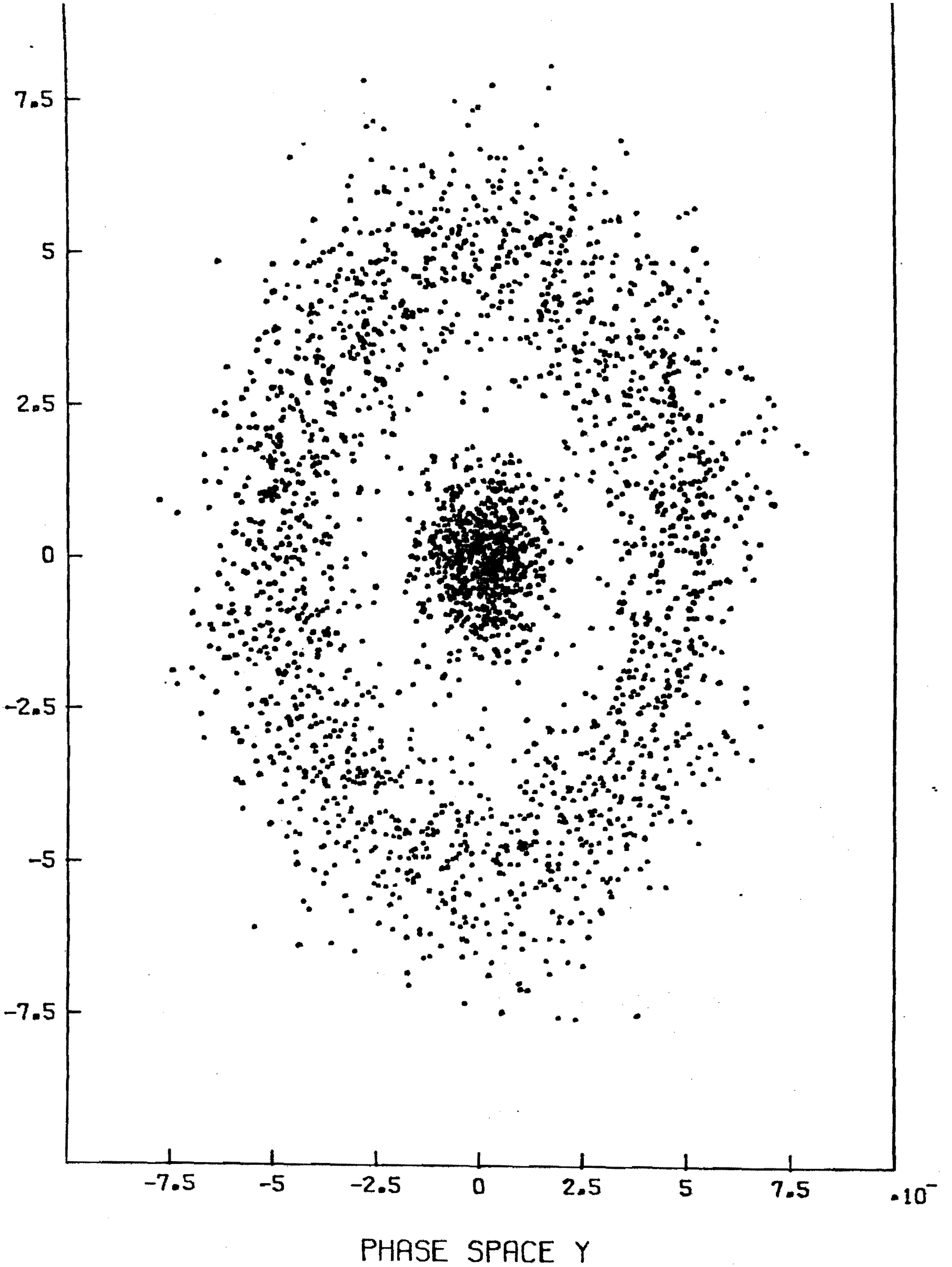

Fig. 7c

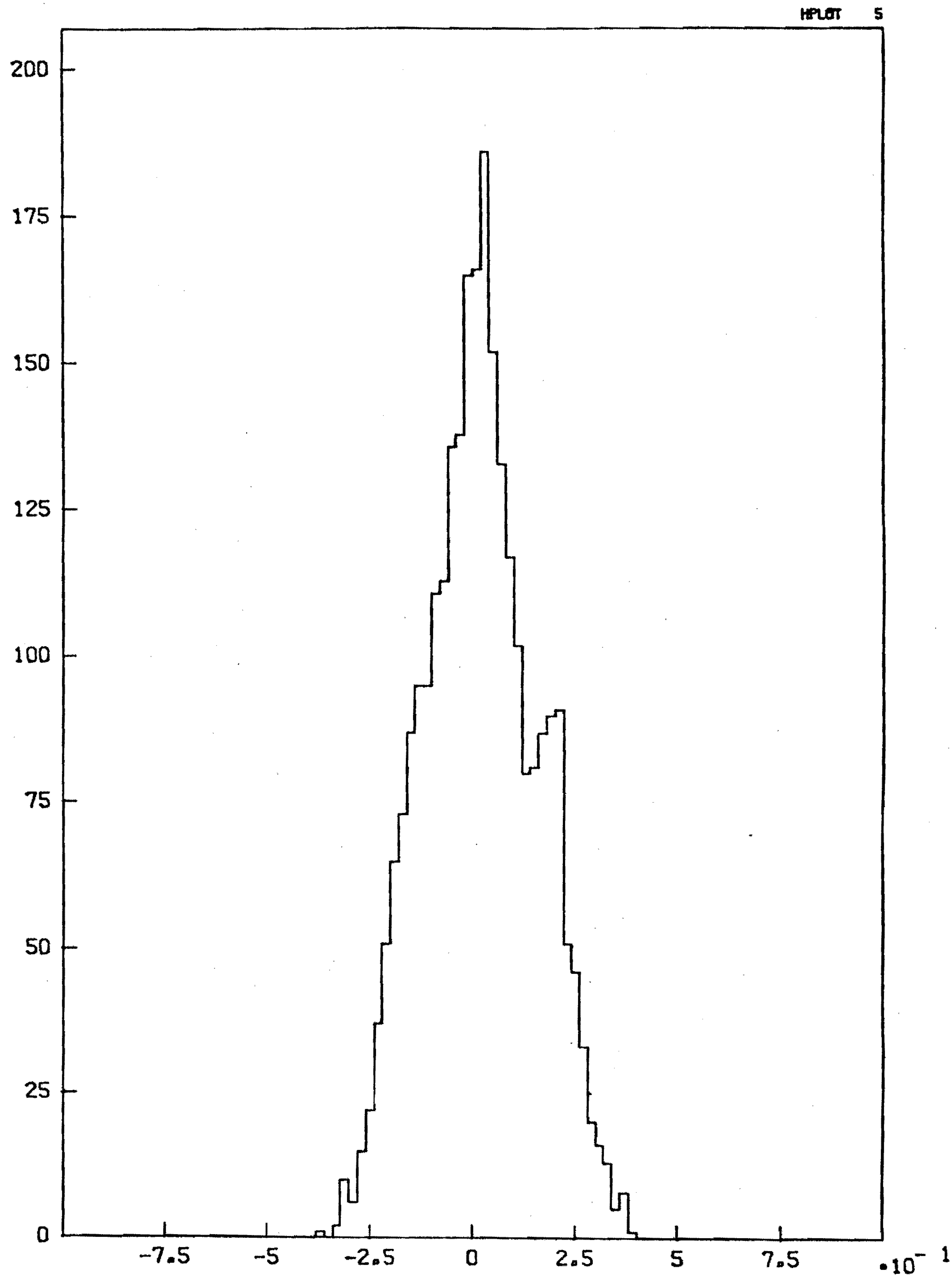

PHASE SPACE X

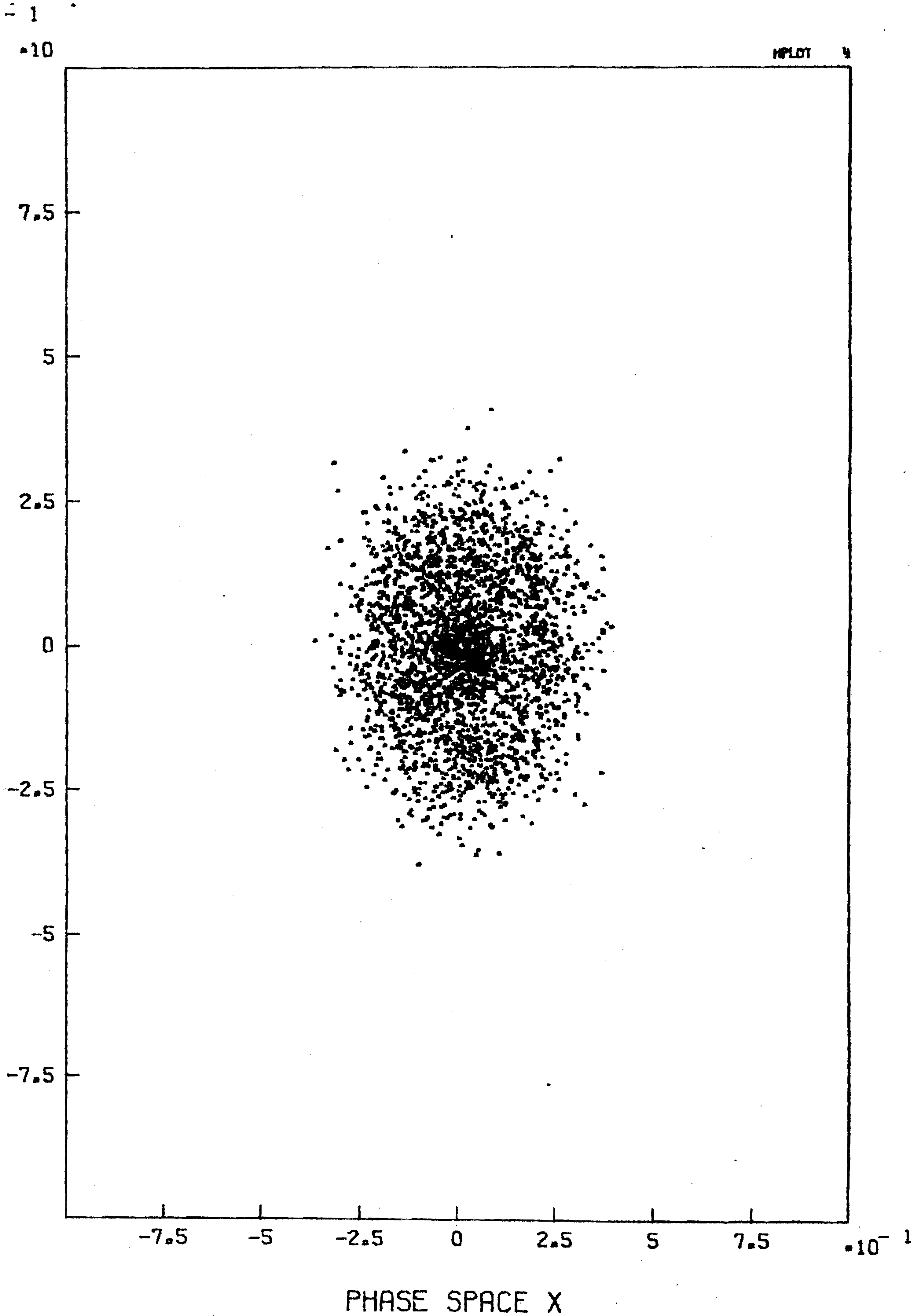

Fig. 7d

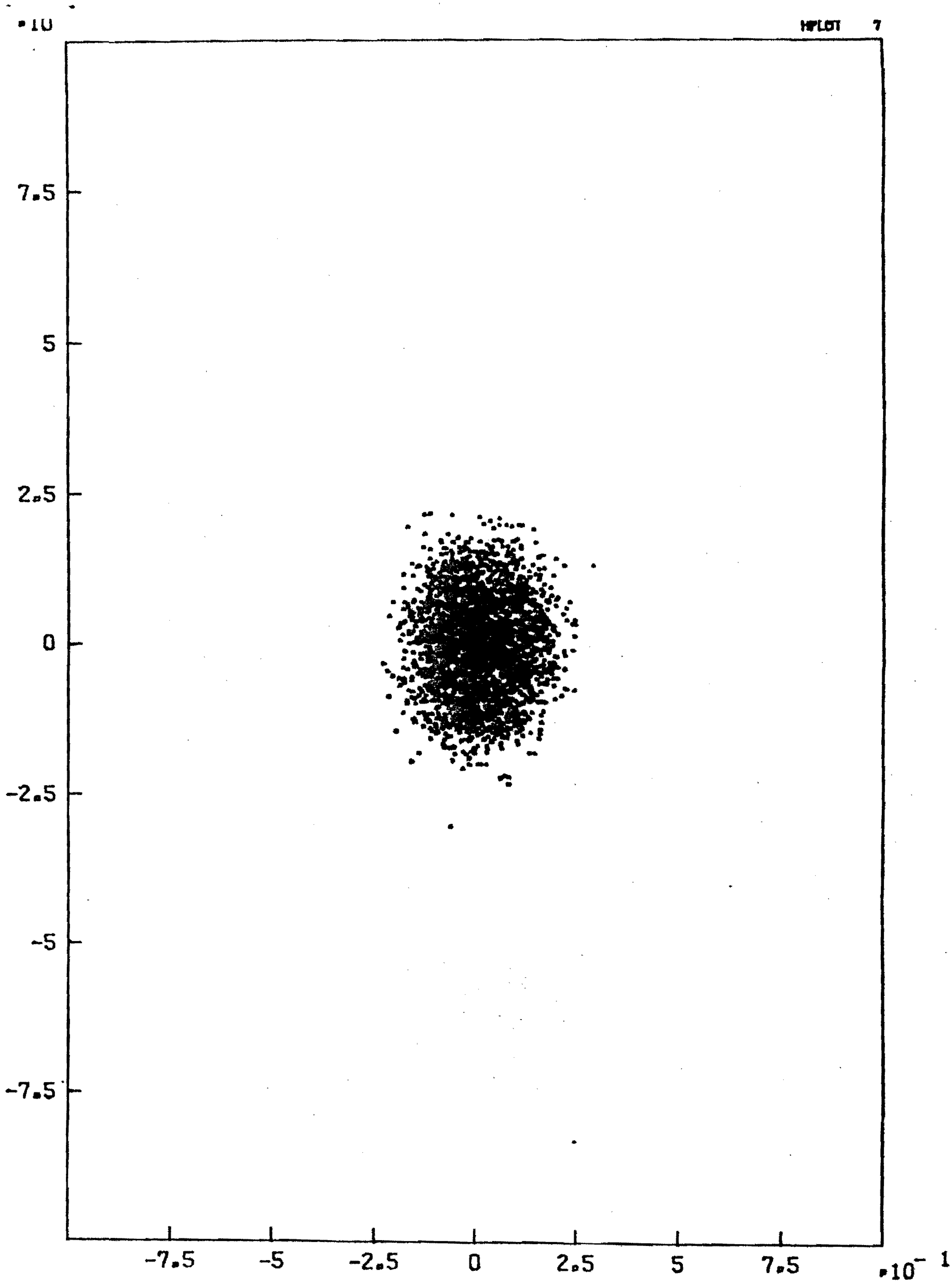

PHASE SPACE X

Fig. 7e

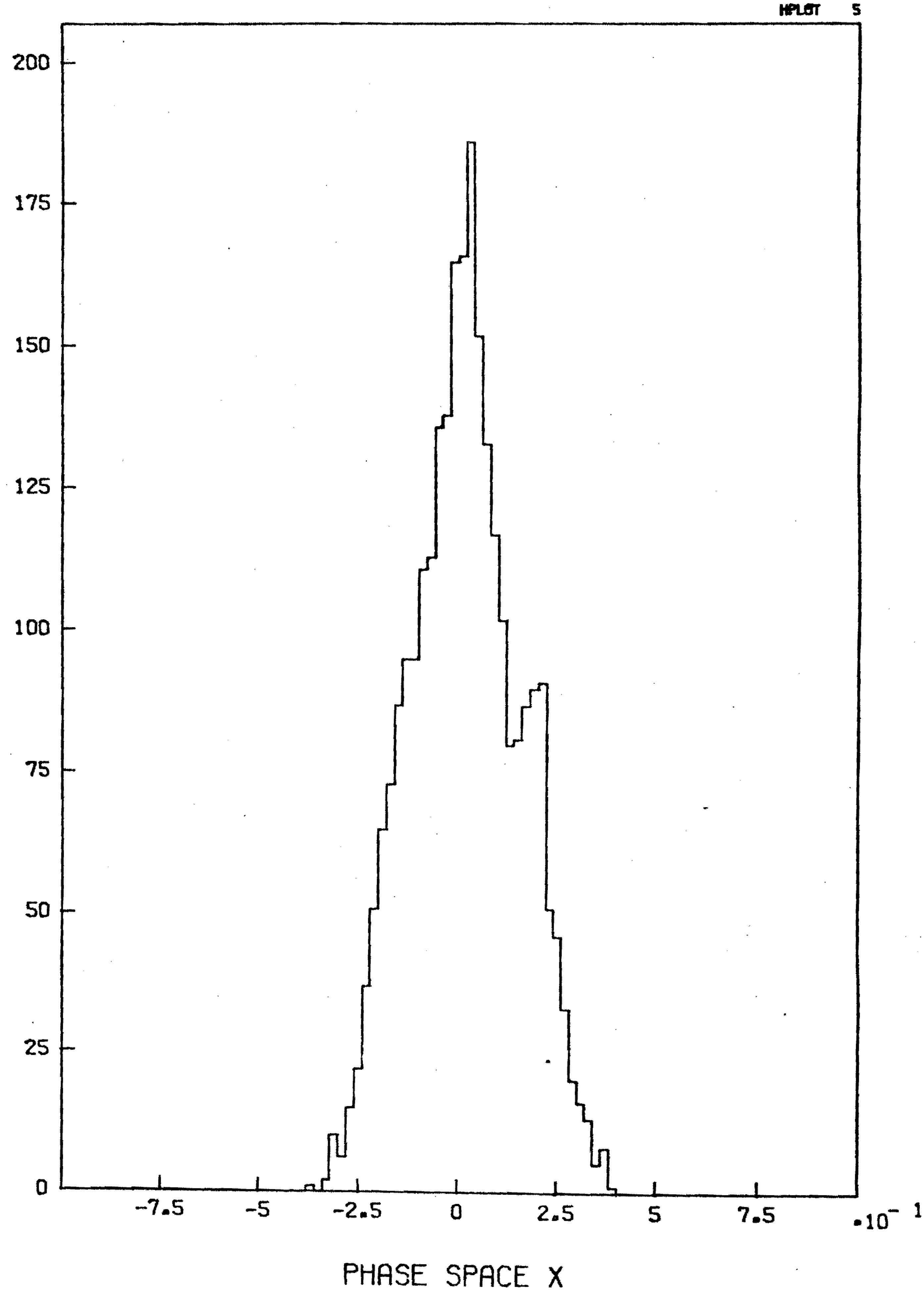

HPLOT 5
200
175
150
125
100
75
50
25
0
-7.5
-5
-2.5
0
2.5
5
7.5
•10⁻ 1
PHASE SPACE X

Fig. 7e

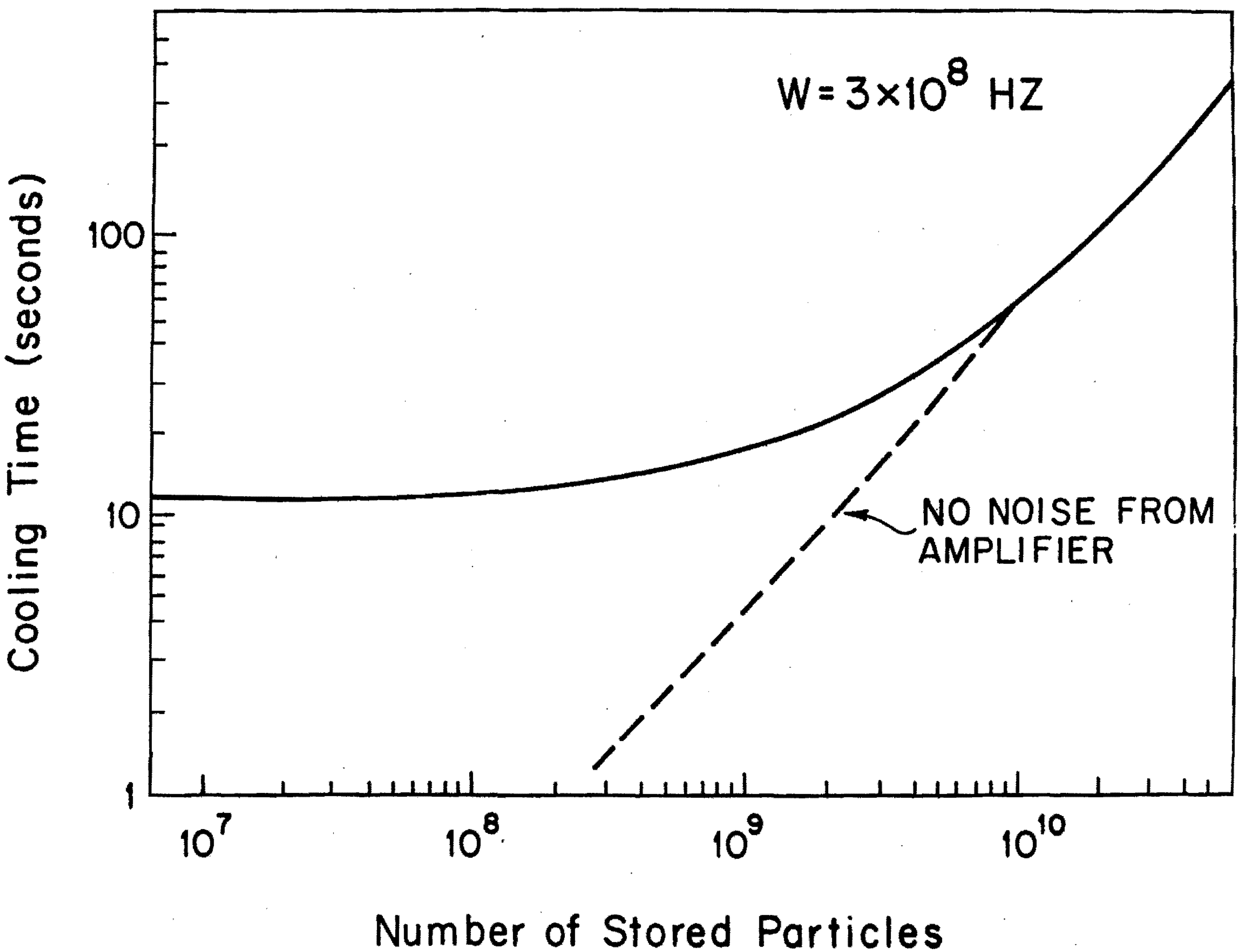

W = 3×10^8 HZ
Cooling Time (seconds)
100
10
1
NO NOISE FROM AMPLIFIER
10^7
10^8
10^9
10^10
Number of Stored Particles

Fig 8

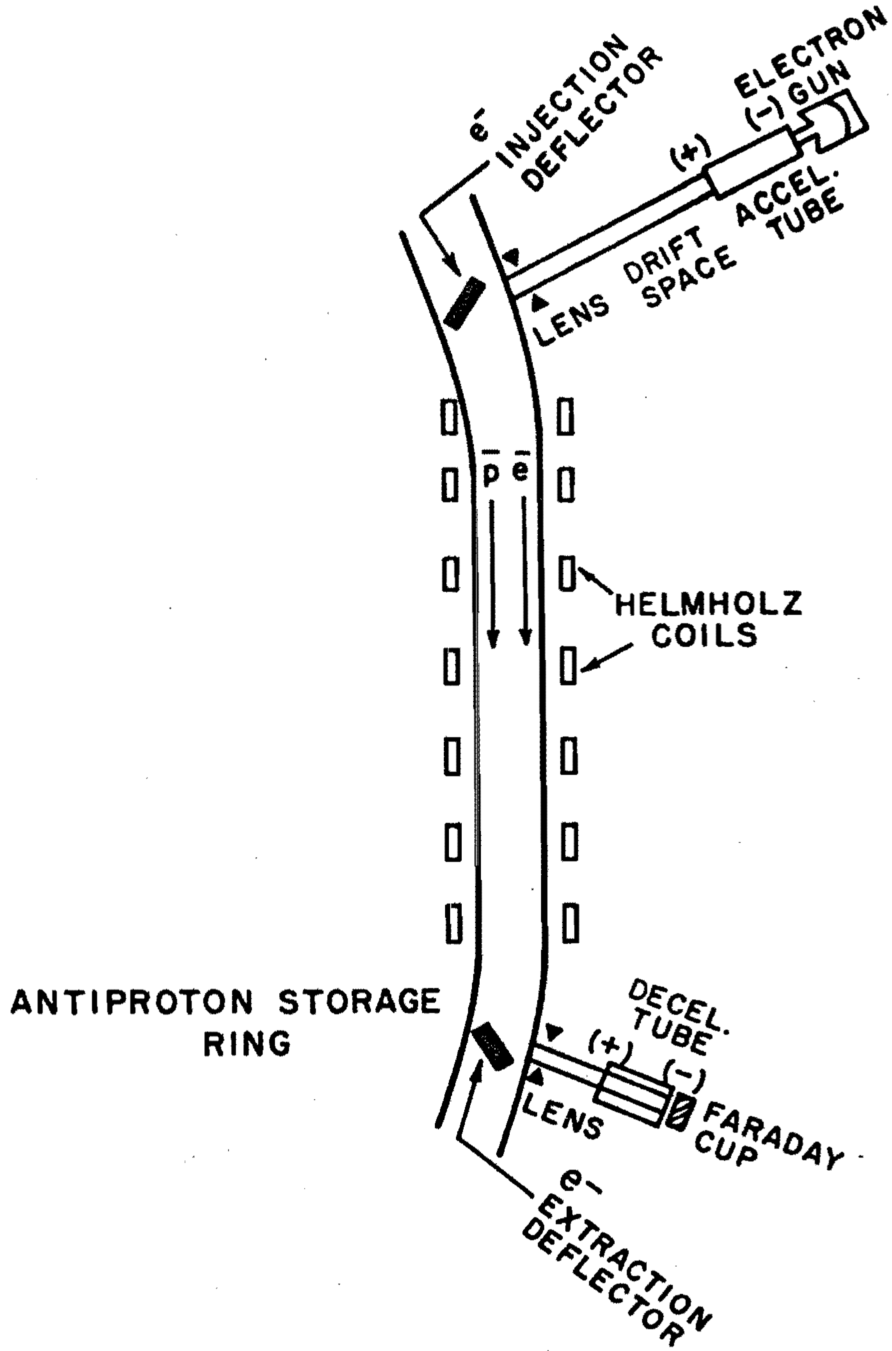

ELECTRON COOLING
STRAIGHT SECTION

Fig 9

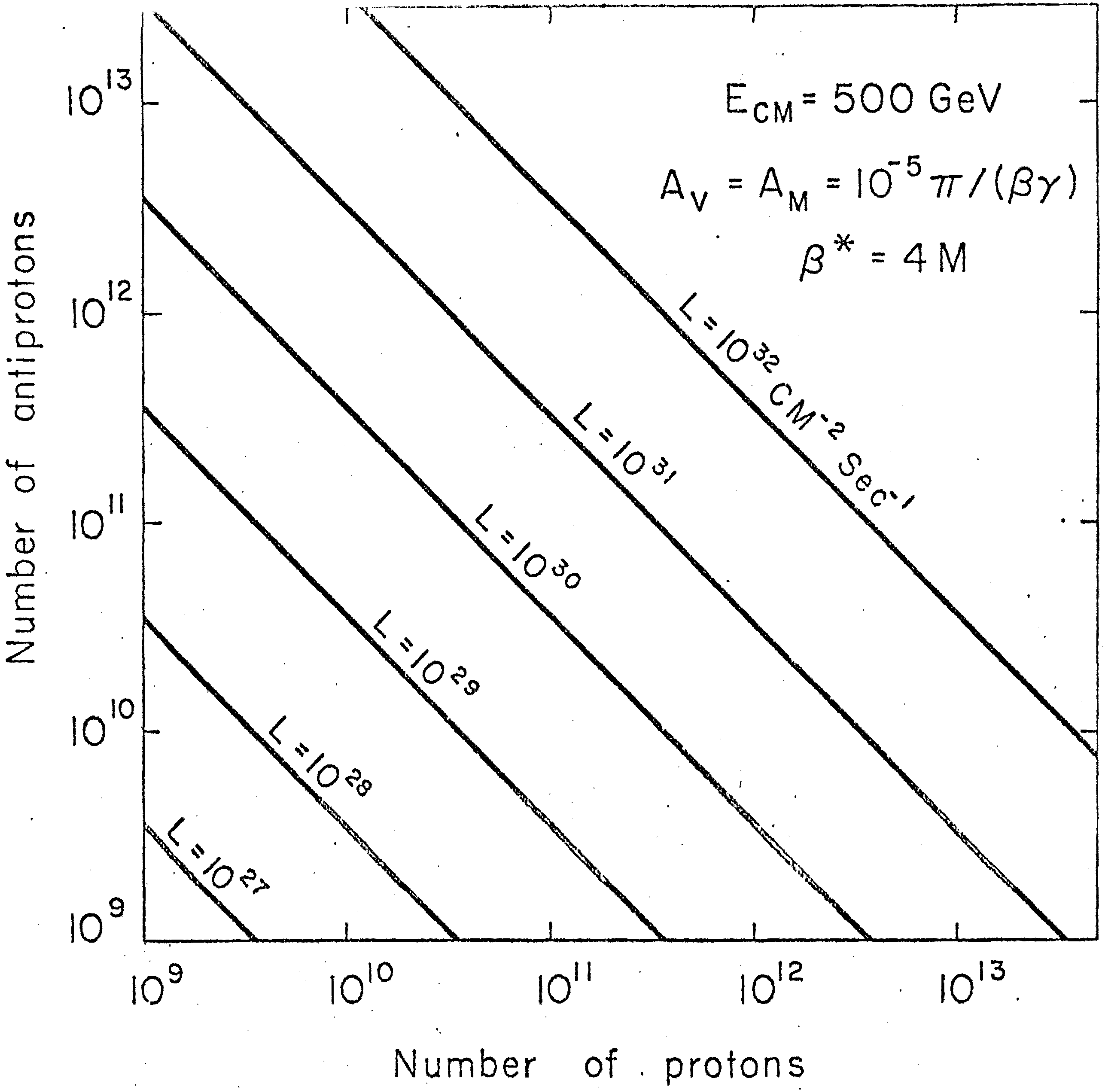

E_{CM} = 500 GeV
$A_V = A_M = 10^{-5}\pi/(\beta\gamma)$
$\beta^* = 4$ M
L = 10^{32} CM^{-2} Sec^{-1}
L = 10^{31}
L = 10^{30}
L = 10^{29}
L = 10^{28}
L = 10^{27}
10^{9}
10^{10}
10^{11}
10^{12}
10^{13}
Number of antiprotons
Number of protons